

Effect of CeO_2 on supported Pd catalyst in the SCR of NO: a DRIFT study

Zhen-lin Liu, Yi-lu Fu*, Jing Tu, and Ming Meng

Department of Chemical Physics, University of Science and Technology of China, Hefei 230026, PR China

Received 14 January 2002; accepted 27 March 2002

The activity of $\text{Pd}/\text{Al}_2\text{O}_3$ and $\text{Pd}/\text{Al}_2\text{O}_3\text{--CeO}_2$ samples has been tested in the selective catalytic reduction of NO by propene. It is found that the activity of $\text{Pd}/\text{Al}_2\text{O}_3$ decreases with calcination temperature, while the activity of $\text{Pd}/\text{Al}_2\text{O}_3\text{--CeO}_2$ increases abnormally with increasing calcination temperature. Surface-area measurement shows both samples suffer a linear decrease in their surface area, so it is reasonable to attribute the activity enhancement to the effect of CeO_2 . The adsorption behavior and state of surface-active sites have been characterized by diffuse reflectance FTIR spectroscopy using CO and NO as probes and the effect of CeO_2 has been revealed. The CeO_2 component increases and stabilizes the dispersion of surface Pd species to prevent it from aggregating at high temperature. CeO_2 may also act as a buffer during the redox cycle of Pd, lengthen the period of Pd redox procedure and render Pd a property of “inertia” in its redox process, thus increasing the activity of the $\text{Pd}/\text{Al}_2\text{O}_3\text{--CeO}_2$ sample. The essential feature of both effects is the strong interaction between Pd and CeO_2 . The intensity of interaction increases linearly with calcination temperature and so does the sample activity.

KEY WORDS: Pd catalysts; CeO_2 effect; calcination temperature; NO SCR; DRIFT.

1. Introduction

The catalytic abatement of NO_x in automobile exhausts is a key problem in controlling air pollution. The conventional three-way catalyst (TWC) can simultaneously remove the CO, C_xH_y and NO_x near the stoichiometry point in the emission. Noble metals are the main component of the catalytic converter. But recently, with the more and more widely used “lean-burn” engine and the diesel engine, the oxidant-to-reductant ratio in the exhaust is not in the operation range of the three-way catalyst, which can only tolerate mild fluctuation of the oxidant/reductant ratio. It becomes a new topic for removing NO_x in an oxidant-rich atmosphere.

Palladium was always used as one of the components of the three-way catalyst, and now Pd-based catalyst is receiving more and more interest in the selective catalytic reduction (SCR) of NO for its high activity, selectivity and abundant availability. Some researchers concentrated their attention on different supports. Desorme *et al.* [1] tested the activity of Pd ion-exchanged mordenite in the SCR of NO. Ali *et al.* [2] and Lobree *et al.* [3] used H-ZSM-5 supported Pd. Pliangos *et al.* [4] studied the effect of YSZ (yttria-stabilized zirconia) supports on the performance of Pd. Besides increasing the dispersion of Pd, providing more surface-active sites, supports have other effects. Ali *et al.* [2] studied the state of Pd on H-ZSM-5 and other acidic supports. They found that with low Pd loading and over acidic

support, the Pd particles are transformed into Pd^{2+} ions, which seems to be necessary for NO reduction. Lobree *et al.* [3] studied the mechanism of NO reduction by CH_4 over Pd–H-ZSM-5. They concluded that the adsorbed NO reacts with CH_4 above 650 K and CN species act as intermediates. They thought that the principal component in Pd–H-ZSM-5 is Pd^{2+} , in agreement with the results of Ali *et al.* Adelman and Sachtler [5] thought Pd^{2+} ions are needed for SCR of NO. However, Pd^{2+} and PdO have similar activity for C_xH_y oxidation with O_2 . The protons are not only required to convert PdO to Pd^{2+} , but also the H^+ and Pd^{2+} act as a bifunctional catalyst.

Effects of different promoters on Pd-only catalysts have also been tested. The alkaline and alkaline earth metals can improve the property of catalysts in adsorbing NO. Yentenakis *et al.* [6] and Yeh *et al.* [7] used Na^+ as promoter. Zirconia and rare earth metal oxides, such as La_2O_3 and CeO_2 , are also used as promoters [8,9], for they can effectively modify catalysts’ surface structure and prevent catalysts from sintering. In particular, much of the literature reported the use of CeO_2 , because of its ability in oxygen storage, which makes the catalysts always maintain high performance despite fluctuations of O_2 in lean-burn engines [10–12]. Sachtler *et al.* [13] found that there exists strong interaction between Pd and CeO_2 .

In our previous study [14], we found that the activity of an aged $\text{Pd}/\text{Al}_2\text{O}_3\text{--CeO}_2$ sample is abnormally higher than the fresh one. In this paper, the effect of calcination temperature on the performance of $\text{Pd}/\text{Al}_2\text{O}_3\text{--CeO}_2$ catalyst has been systematically tested. The adsorption

* To whom correspondence should be addressed.

behavior and state of surface-active sites have been characterized by diffuse reflectance FTIR spectroscopy using CO and NO as probes and the possible reason for the activity enhancement has been discussed.

2. Experimental

Pd/ Al_2O_3 – CeO_2 catalysts with an Al/Ce ratio of 4:1 were prepared by successively impregnating Al_2O_3 with $\text{Ce}(\text{NO}_3)_3$ and PdCl_2 solution. The products were then dried overnight at 110 °C and air-calcined at 500 °C for 2 h. This sample was designated as Pd/Al–Ce. For comparison, Pd/ Al_2O_3 catalysts were also prepared, and designated as Pd/Al. Each sample was divided into four parts and calcined at 600, 700, 800 and 900 °C respectively. The surface areas of samples calcined at elevated temperature are measured by the BET method.

Activity tests were performed in a flow system, which consists of a feed unit, a stainless steel microreactor with 6 mm i.d., on-line gas chromatograph (Model SC-6) with FID detector and chemiluminescence nitrogen oxides analyzer (Model 8840). A sample of 1 ml was reduced in an H_2 stream at 500 °C for 2 h before activity test. Reactants (NO 0.08%, C_3H_6 0.12%, O_2 1.8%) and balance gas N_2 were supplied *via* mass flow controllers.

The diffuse reflectance infrared Fourier transform (DRIFT) spectra were recorded with a resolution of 4 cm^{-1} on a Nicolet 460 E.S.P. spectrometer supplied with a diffuse reflectance attachment. The probe gases, NO and CO, were of high purity (99.99%) and were used as supplied. Sample powder (0.18–0.15 mm) was filled in a self-made quartz DRIFT cell with a CaF_2 window. Prior to measurement, samples were evacuated at 450 °C for 5 h, cooled to room temperature and then exposed to CO. When the spectra were taken, samples were again evacuated at 450 °C, then exposed to NO for DRIFT measurement.

3. Results and discussion

3.1. Surface-area measurement and activity test

Table 1 lists the surface area of samples calcined at elevated temperature. It can be seen, for both

Table 1
The surface area data of samples at different calcination temperatures

Samples	Surface area (m^2/g)			
	600 °C	700 °C	800 °C	900 °C
Pd/Al	139.6	136.1	118.6	112.1
Pd/Al–Ce	70.5	60.3	54.4	38.8

Pd/ Al_2O_3 – CeO_2 and Pd/ Al_2O_3 samples, that the surface area decreases linearly with temperature. We use the highest NO conversion to characterize the activity of samples in the NO SCR reaction. The data are listed in table 2. For Pd/ Al_2O_3 , the activity decreases as a whole when calcination temperature is raised. This may be due to the surface sintering. But for Pd/ Al_2O_3 – CeO_2 samples, the activity increases linearly when calcination temperature is raised from 600 to 900 °C. Some Pd/ Al_2O_3 – CeO_2 samples were also prepared by the sol-gel method and calcined at different temperature, and same activity enhancement was observed [15]. From table 1, it can be seen that Pd/ Al_2O_3 – CeO_2 samples also suffer a shrinkage in surface area, so it is reasonable to ascribe the activity enhancement at high calcination temperature to the effect of CeO_2 .

3.2. CO adsorption

Figure 1 presents the spectra recorded after CO adsorption on a fresh (air-calcined at 500 °C for 2 h) Pd/Al sample. All spectra were referenced to those of the blank sample. Upon CO adsorption at room temperature (RT) (figure 1(a)), a weak band at 2200 cm^{-1} is observed, which is removed after evacuation at RT. It may be attributed to CO weakly held on the surface. Three strong bands, which are resistant to evacuation, are observed in the region of linearly adsorbed CO, centered at 2160, 2125 and 2100 cm^{-1} , respectively. Lokhov and Davydov [16] substantiated that the frequency for M^{2+}CO is above 2170 cm^{-1} , M^+CO in the region of 2120–2160 cm^{-1} , and M^0CO below 2100 cm^{-1} . The bands at 2160 and 2125 cm^{-1} may be assigned to CO adsorbed on cationic Pd^{2+} with different sites, and the band at 2100 cm^{-1} responds to CO adsorbed on metal state Pd^0 [17–20]. On fresh Pd/Al samples, surface Pd species should be mainly in the cationic state Pd^{2+} .

Table 2
The highest NO conversion and the corresponding temperatures of samples calcined at different temperatures

Samples	600 °C		700 °C		800 °C		900 °C	
	Conversion (%)	Temperature (°C)						
Pd/Al	25.3	310	24.5	310	25.3	310	23.5	310
Pd/Al–Ce	22.9	310	24.7	310	32.2	290	40.3	270

GHSV = 30 000 h^{-1} .

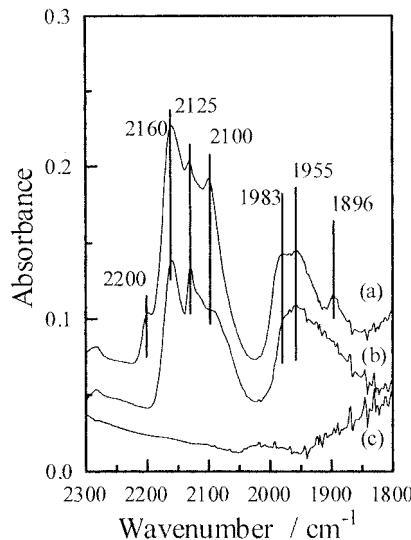


Figure 1. DRIFT spectra of CO adsorbed on fresh Pd/Al_2O_3 . (a) RT, 100 Torr, (b) RT, 10^{-2} Torr, (c) $350^\circ C$, 10^{-2} Torr.

after being air-calcined at $500^\circ C$. But Pd^{2+} may go through self-reduction in the pre-evacuation at $450^\circ C$. Prior to CO adsorption, there may be both Pd^{2+} and Pd^0 on the surface, so bands of CO adsorbed on both sites are presented. In fact, the self-reduction of Pd^{2+} was observed even when evacuated at RT in our experiment. The band between 1983 and 1955 cm^{-1} is related to two-fold bridge-bonded CO on surface Pd^0 species [21,22]. This band is broadened, indicating the complexity of Pd sites, such as $Pd^{\delta+}$. The band at 1896 cm^{-1} possibly corresponds to three-fold bridge-bonded CO [23].

After evacuation at RT (figure 1(b)), the band at 1983 cm^{-1} is weakened to a shoulder, and a band centered at 1955 cm^{-1} appears. This indicates that some $Pd^{\delta+}$ may become Pd^0 [24]. The band at 1896 cm^{-1} is also weakened to a shoulder.

Figure 2 shows the spectra of CO adsorbed on a fresh $Pd/Al-Ce$ sample. Three bands of linearly-adsorbed CO on Pd sites are also detected at 2160 , 2125 and 2100 cm^{-1} (figure 2(a)). Compared with spectra from the Pd/Al sample (figure 1(a)), there is no difference in the band position, but the band of CO adsorbed on metal state Pd^0 is much weaker, which appears as a shoulder. This seems to indicate that, though under the same pre-treatment condition, the self-reduction of Pd^{2+} on $Pd/Al-Ce$ samples is not as apparent as on Pd/Al samples. We argue that the strong interaction of $Pd-CeO_2$ inhibits the self-reduction of Pd^{2+} . The two-fold bridge-bonded CO gives rise to two bands at 2014 and 1962 cm^{-1} . The blue-shift of these two bands (compared with bands at 1983 and 1955 cm^{-1} , figure 1(a)) may also be ascribed to the strong interaction of $Pd-CeO_2$, which makes $Pd^{\delta+}$ hold more positive charge. After evacuation, the band at 2014 cm^{-1} disappears and the band at 1962 cm^{-1} is weakened to a shoulder, and a broad feature centered at 1945 cm^{-1} appears.

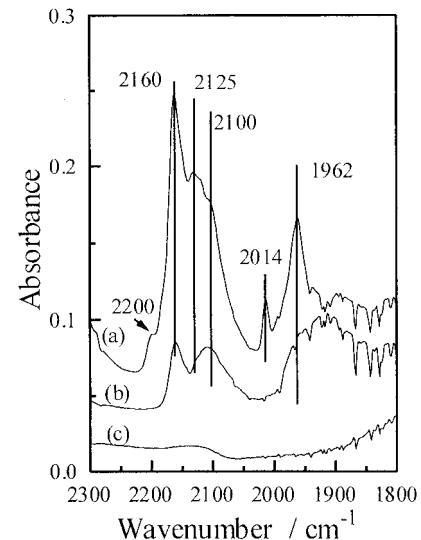


Figure 2. DRIFT spectra of CO adsorbed on fresh $Pd/Al_2O_3-CeO_2$. (a) RT, 100 Torr, (b) RT, 10^{-2} Torr, (c) $350^\circ C$, 10^{-2} Torr.

Figure 3 shows the spectra of CO adsorbed on a reduced (in H_2 at $450^\circ C$ for 2 h) Pd/Al sample. Linearly-adsorbed CO gives rise to a strong band at 2100 cm^{-1} , and a very weak shoulder at 2160 cm^{-1} . This implies that the surface Pd^{2+} cations are not completely reduced by H_2 at $450^\circ C$. Furthermore, part of the Pd may hold a positive charge, broadening the band at 1979 cm^{-1} . After evacuation, the bands at 2100 and 1979 cm^{-1} shift to 2076 and 1929 cm^{-1} , respectively. A possible cause of the red-shift is that Pd accepts electrons from CO and holds less positive charge.

Figure 4 presents the spectra recorded from CO adsorption on a fresh $Pd/Al-Ce$ sample. Compared with Pd/Al , CO linearly adsorbed on the $Pd/Al-Ce$ sample gives a much stronger band at 2170 cm^{-1} ,

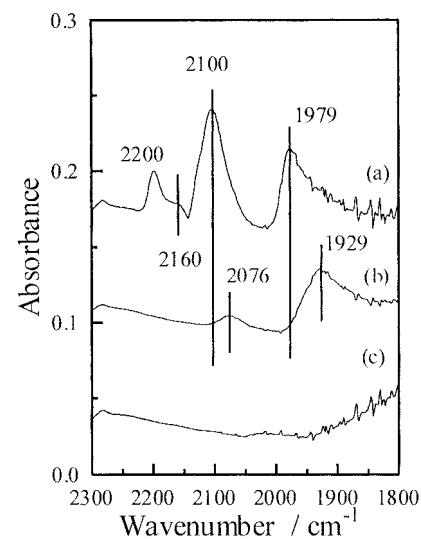


Figure 3. DRIFT spectra of CO adsorbed on reduced Pd/Al_2O_3 . (a) RT, 100 Torr, (b) RT, 10^{-2} Torr, (c) $350^\circ C$, 10^{-2} Torr.

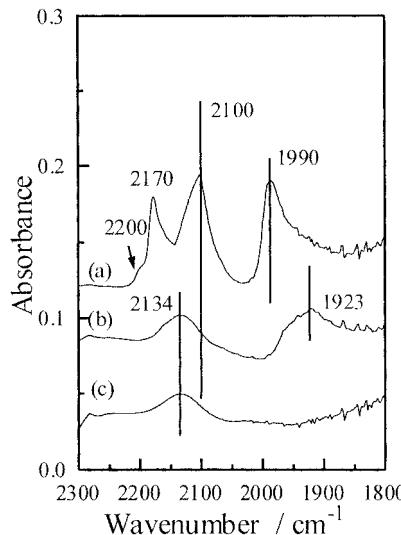


Figure 4. DRIFT spectra of CO adsorbed on reduced $\text{Pd}/\text{Al}_2\text{O}_3-\text{CeO}_2$. (a) RT, 100 Torr, (b) RT, 10^{-2} Torr, (c) 350°C , 10^{-2} Torr.

which relates to the Pd^{2+} -CO species. This implies CeO_2 effectively inhibits the reduction of Pd^{2+} by H_2 . Investigations of CeO_2 redox properties [25–27] show that, in a reducing environment, reduction of surface CeO_2 occurs at 600 – 720 K , and reduction of bulk CeO_2 occurs at 720 – 900 K , which forms CeO_{2-x} ($0 < x < 0.5$). When bulk CeO_2 is reduced, it loses some lattice O atoms, but still maintains the CaF_2 -type structure, with large numbers of O defect sites. This CeO_{2-x} with O defect sites is not stable: it can be reoxidized to form CeO_2 at RT [27–29]. Under the applied experiment conditions, it is possible that only part of the bulk CeO_2 is reduced. Because of the strong interaction between Pd and CeO_2 , part of the Pd also maintains its original oxidation state and is not reduced by H_2 . Thus, the band at 2170 cm^{-1} corresponding to the Pd^{2+} -CO becomes much stronger. After evacuation, bands at 2170 and 2100 cm^{-1} are weakened to shoulders, and a broad band centered at 2134 cm^{-1} appears. This is different on the Pd/Al sample (figure 3(b), band at 2076 cm^{-1}). We concluded that the strong interaction of Pd- CeO_2 decreases the electron density on Pd, and that Pd donates fewer electrons to the anti-bonding π molecular orbital of CO, which results in the blue-shift on CO absorption band.

Figures 5 and 6 present the spectra of CO adsorbed on aged Pd/Al and Pd/Al-Ce samples, respectively. On the aged Pd/Al sample, two very weak bands are observed at 2120 and 1995 cm^{-1} , corresponding to linearly-adsorbed CO and bridge-bonded CO. The two bands disappear after evacuation at RT. When air-calcined at 900 °C for 2 h, the Pd/Al sample suffers severe sintering. Pd species aggregate and form PdO particles, which only weakly adsorb CO molecules. On the aged Pd/Al-Ce sample, two bands with moderate intensity are observed at 2100 and 1990 cm^{-1} , in the same position as bands for the reduced Pd/Al-Ce sample. This indicates that CeO_2 can greatly increase the stability of surface Pd

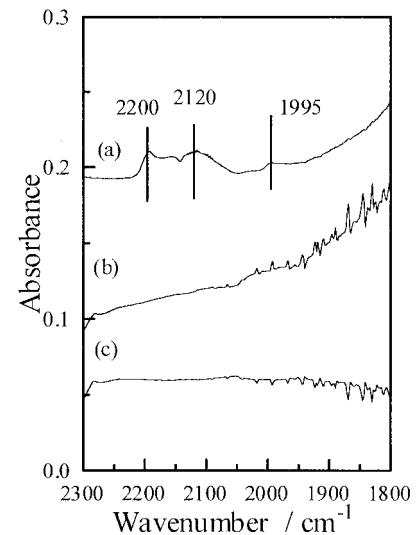


Figure 5. DRIFT spectra of CO adsorbed on aged $\text{Pd}/\text{Al}_2\text{O}_3$. (a) RT, 100 Torr, (b) RT, 10^{-2} Torr, (c) 350°C , 10^{-2} Torr.

species, and prevent Pd from aggregation at temperatures as high as 900 °C .

3.3. NO adsorption

Figure 7 shows the spectra of NO adsorbed on the fresh Pd/Al sample. A band at 2236 cm^{-1} is observed, which is removed upon evacuation at RT. It is attributed to N_2O species formed during the dissociative adsorption of NO on Pd [21]. The band located at 1753 cm^{-1} is related to NO adsorbed on metallic Pd. A shoulder at 1808 cm^{-1} corresponds to NO adsorbed on cationic Pd^{2+} [24]. After evacuation at RT, the relative intensity of these two bands changes drastically. The band at 1808 cm^{-1} dominates and the band at 1753 cm^{-1} is weakened to a shoulder.

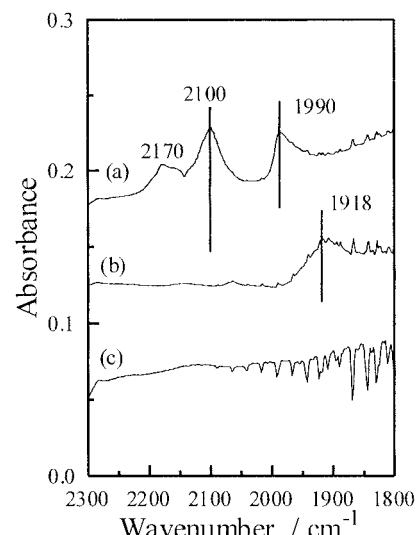


Figure 6. DRIFT spectra of CO adsorbed on aged $\text{Pd}/\text{Al}_2\text{O}_3-\text{CeO}_2$. (a) RT, 100 Torr, (b) RT, 10^{-2} Torr, (c) 350°C , 10^{-2} Torr.

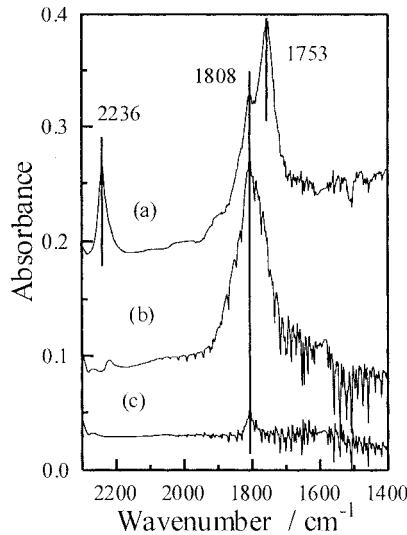


Figure 7. DRIFT spectra of NO adsorbed on fresh $\text{Pd}/\text{Al}_2\text{O}_3$. (a) RT, 100 Torr, (b) RT, 10^{-2} Torr, (c) 350°C , 10^{-2} Torr.

Figure 8 shows the spectra of NO adsorbed on a fresh Pd/Al–Ce sample. A strong, broad band centered at 1786 cm^{-1} is observed. After evacuation at RT and 200°C , the intensity of this band slightly decreases, but no frequency shift is observed. Bands between 1573 and 1538 cm^{-1} are assigned to surface nitrate species. A band at 1697 cm^{-1} appears after evacuation at RT. It may relate to bent NO species $\text{Pd}-\text{NO}^-$ [24].

As described above, there are both Pd^{2+} and Pd^0 species on the catalyst surface, so the adsorption of NO on Pd/Al gives rise to two bands at 1808 and 1753 cm^{-1} , corresponding to $\text{Pd}^{2+}-\text{NO}$ and Pd^0-NO species, respectively. As an oxidant, NO can oxidize Pd^0 to Pd^{2+} during its adsorption [3]. This argument can be verified by the appearance of N_2O , which is a dissociative adsorption

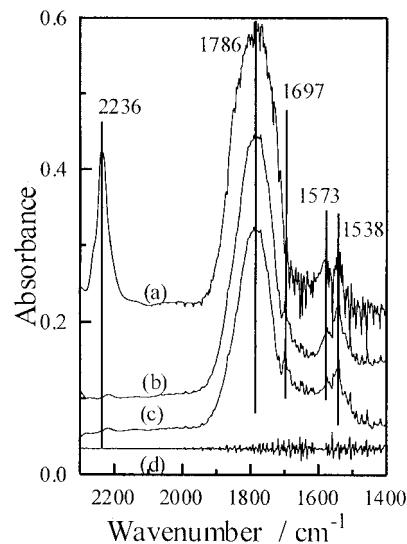


Figure 8. DRIFT spectra of NO adsorbed on fresh $\text{Pd}/\text{Al}_2\text{O}_3-\text{CeO}_2$. (a) RT, 100 Torr, (b) RT, 10^{-2} Torr, (c) 200°C , 10^{-2} Torr, (d) 350°C , 10^{-2} Torr.

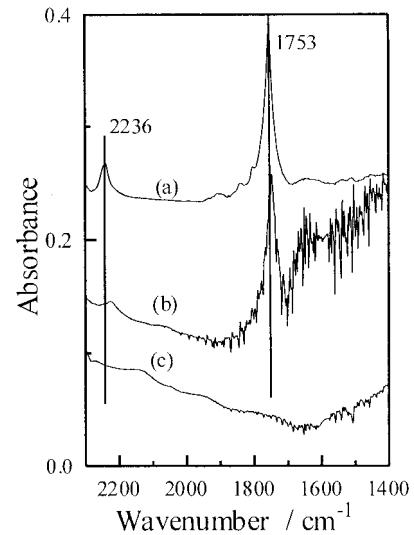


Figure 9. DRIFT spectra of NO adsorbed on reduced $\text{Pd}/\text{Al}_2\text{O}_3$. (a) RT, 100 Torr, (b) RT, 10^{-2} Torr, (c) 350°C , 10^{-2} Torr.

product of NO. There exist adsorbed O atoms on the surface. On the Pd/Al sample, this oxidation reaction proceeds smoothly, and the band related to Pd^0-NO decreases, while the band related to $\text{Pd}^{2+}-\text{NO}$ increases. But on the fresh Pd/Al–Ce sample, bands of $\text{Pd}^{2+}-\text{NO}$ and Pd^0-NO overlap and form a broad band centered at 1786 cm^{-1} . No change in the band shape is detected, so no change in the relative intensity of these two bands occurs. This again verifies that CeO_2 gives Pd a property to resist oxidizing.

Figure 9 presents the spectra recorded from the adsorption of NO on the reduced Pd/Al sample. A sharp band at 1753 cm^{-1} corresponds to NO adsorbed on metallic Pd. This band does not change its position when evacuated. On the reduced Pd/Al–Ce sample (figure 10), a band at

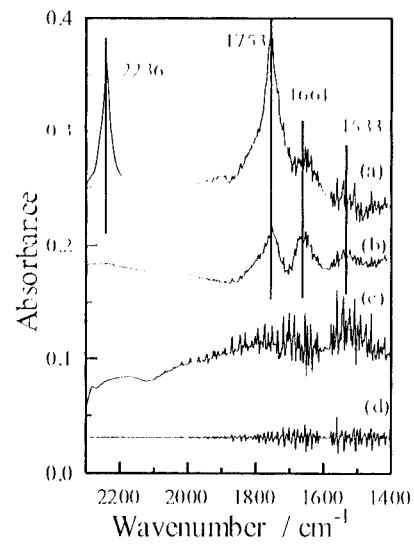


Figure 10. DRIFT spectra of NO adsorbed on reduced $\text{Pd}/\text{Al}_2\text{O}_3-\text{CeO}_2$. (a) RT, 100 Torr, (b) RT, 10^{-2} Torr, (c) 200°C , 10^{-2} Torr, (d) 350°C , 10^{-2} Torr.

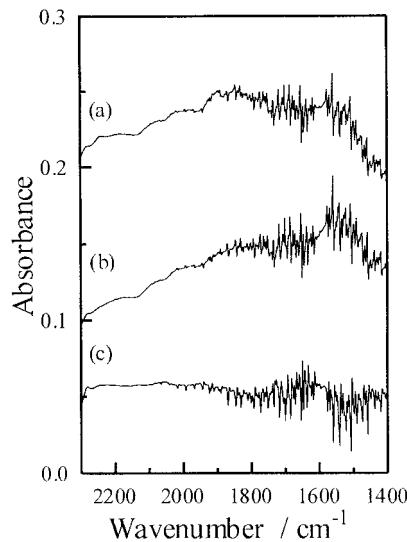


Figure 11. DRIFT spectra of NO adsorbed on aged $\text{Pd}/\text{Al}_2\text{O}_3$. (a) RT, 100 Torr, (b) RT, 10^{-2} Torr, (c) 350°C , 10^{-2} Torr.

1753 cm^{-1} is also observed, and a band related to bent $\text{Pd}-\text{NO}^-$ species is located at 1661 cm^{-1} .

On the aged Pd/Al sample (figure 11), there is no distinguishable band of NO adsorption, while on the aged Pd/Al–Ce sample (figure 12), bands at 2236 , 1839 and 1613 cm^{-1} are still observed, though with low intensity. This also verifies that CeO_2 may increase the stability of surface Pd species and prevent Pd from aggregation at 900°C .

3.4. Promoter effects of CeO_2

In three-way catalysis, CeO_2 promotes the catalyst performance by adjusting the O_2 concentration and keeping the air/fuel ratio in the operation range of catalyst. But the oxygen storage property may not be simply and directly applied to explain the activity increase of Pd/Al–Ce sample with increasing calcination temperature. It is possible that CeO_2 affects the catalyst performance in both structural and electric aspects.

Firstly, CeO_2 may act as a structure promoter. It efficiently enhances the dispersion of Pd species and prevents Pd from aggregation at 900°C . This can be deduced from comparing the IR spectra of CO and NO adsorbed on aged Pd/Al and Pd/Al–Ce samples. CO is weakly held on the aged Pd/Al surface, and it desorbs readily after evacuation at RT, while on the aged Pd/Al–Ce sample, bands are of moderate intensity, and are located at the same position as bands on the reduced Pd/Al–Ce sample. A very similar result has been observed by Sachtler and co-workers [13]. They report that Pd is easily oxidized upon exposure to air for the CeO_2 -promoted Pd catalysts, which reflects a higher metal dispersion of Pd anchored on ceria. CeO_2 interacts strongly with Pd, either by forming Pd– CeO_2 clusters or by introducing Pd into the lattice of CeO_2 [30]. The NO

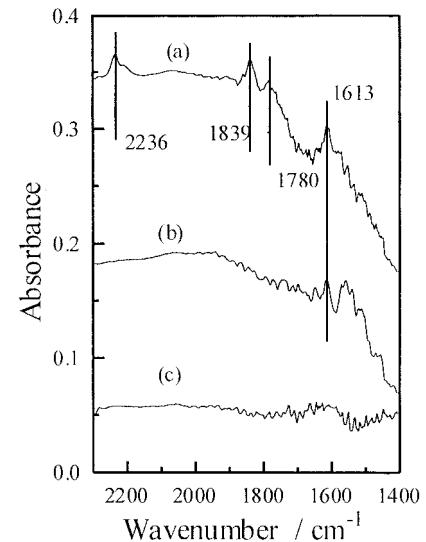


Figure 12. DRIFT spectra of NO adsorbed on aged $\text{Pd}/\text{Al}_2\text{O}_3-\text{CeO}_2$. (a) RT, 100 Torr, (b) RT, 10^{-2} Torr, (c) 350°C , 10^{-2} Torr.

adsorption on the aged Pd/Al surface is even weaker than CO adsorption, and no distinguishable band of NO adsorption is found. On the aged Pd/Al–Ce sample, bands of NO adsorption can still be distinguished.

Secondly, because of the strong interaction of Pd– CeO_2 , CeO_2 may act as a buffer in the redox cycle of Pd and make it difficult to change the oxidation state of Pd. After the addition of CeO_2 , Pd shows a property of “inertia” to keep its original valence. Both the reduction and oxidation of Pd species need longer processes. In a reducing atmosphere, such as during CO adsorption, or under conditions favoring self-reduction, an isolated Pd is readily reduced *via* accepting electrons. On the Pd/Al–Ce sample, CeO_2 decreases the electron density of Pd and keeps Pd in the cationic state. CeO_2 accepts the electrons, loses an O atom and forms the lattice O defect sites. CeO_2 can still maintain its CaF_2 -type structure when losing up to 25% of lattice O atoms in the temperature range 720 – 900 K . By interaction of Pd– CeO_2 , the O-storage property of CeO_2 may greatly increase the ability of Pd to resist reduction. The process from Pd^{2+} to Pd^0 needs more reductant and longer reaction period. In an oxidizing environment, such as during NO adsorption, because of the affinity of CeO_{2-x} to O, the O atoms adsorbed on Pd may spill over to CeO_{2-x} and fill the lattice O defect sites. Pd stays in its metal state. The process from Pd^0 to Pd^{2+} needs more oxidant and a longer reaction period. With addition of CeO_2 , Pd possesses larger redox “capacity”. Thus, CeO_2 exhibits its promoter effect *via* lengthening of the redox cycle of Pd. Sachtler and co-workers [13] observed this kind of effect of ceria on Pd catalyst in another way. They found that Ce^{4+} can be easily reduced to Ce^{3+} at temperatures as low as 300°C for CeO_2 -promoted Pd catalysts, which suggested obviously an interaction between Pd and CeO_2 .

Essentially, this is in accordance with the present result.

Both effects of ceria rise from the interaction between CeO_2 and Pd, which should be considered as a thermodynamic effect. However, when ceria acts as a buffer in the redox cycle of Pd, kinetic effects cannot be excluded. The activity of the Pd/Al₂O₃–CeO₂ sample abnormally increases with calcination temperature. It is possible that, when calcined at high temperature, the surface species migrate and reconstruct to form more Pd–CeO₂ clusters or introduce more Pd into the CeO₂ lattice. The interaction between Pd and CeO₂ becomes stronger and thus increases the activity of the Pd/Al₂O₃–CeO₂ catalyst.

4. Conclusions

As a structural promoter, CeO₂ effectively enhances and maintains the dispersion of Pd on the catalyst surface and prevents Pd from severe aggregation at temperatures as high as 900 °C. On the aged Pd/Al₂O₃ sample, CO and NO are very weakly adsorbed. This suggests that surface Pd species are oxidized completely and aggregate to form relatively big PdO particles, which exhibit no activity in the NO SCR reaction [2]. On the aged Pd/Al₂O₃–CeO₂ sample, bands of moderate intensity are still observed during CO and NO adsorption. This implies that CeO₂ can effectively maintain the dispersion of Pd at high temperature and maintain the activity of the catalyst.

There seems to be strong interaction between Pd and CeO₂, which makes CeO₂ act as a buffer during the redox cycle of Pd. In Pd/Al₂O₃–CeO₂, Pd shows a property of inertia to keep its original oxidation state. Two reasons are proposed to explain this phenomenon. Firstly, the CeO₂ lattice may act as an O atom barrier in the O-rich condition and an O atom reservoir in the O-lean condition, thus counteracting the fluctuation in O concentration and making the local environment of Pd stable. Secondly, the O atoms adsorbed on Pd may spill over to the CeO₂ lattice and leave Pd in the metal state in the O-rich condition; or vice versa, the O atom may diffuse from the CeO₂ lattice to Pd and keep Pd in a cationic state. The oxidation of Pd⁰ to Pd²⁺ needs more O atoms and a longer time, and similarly the reduction of Pd²⁺ to Pd⁰ needs more reductant. The

supported Pd catalyst with a CeO₂ component shows larger redox “capacity” and a longer redox cycle. When calcined at high temperature, the interaction between Pd and CeO₂ becomes stronger and the catalyst shows higher activity at elevated calcination temperatures.

References

- [1] C. Descorme, P. Gelin, C. Lecuyer et al., *J. Catal.* 177 (1998) 352.
- [2] A. Ali, W. Alvarez, C.J. Loughran et al., *Appl. Catal. B* 14 (1997) 13.
- [3] L.J. Lobree, A.W. Aylor, J.A. Reimer et al., *J. Catal.* 181 (1999) 189.
- [4] C. Pliangos, I.V. Yentekakis, V.G. Papadakis et al., *Appl. Catal. B* 14 (1997) 161.
- [5] B.J. Adelman and W.M.H. Sachtler, *Appl. Catal. B* 14 (1997) 1.
- [6] I.V. Yentekakis, R.M. Lambert, M.S. Tikhov et al., *J. Catal.* 176 (1998) 82.
- [7] C.T. Yeh, C.B. Wang, J.G. Chang et al., *Appl. Catal. B* 17 (1998) 51.
- [8] H. Muraki, K. Yokota and Y. Fujitani, *Appl. Catal.* 48 (1989) 93.
- [9] P. Fornasiero, J. Kaspar, V. Sergo et al., *J. Catal.* 182 (1999) 56.
- [10] J.E. Kubsh, J.S. Rieck and N.D. Spencer, *Catalysis and Automotive Pollution Control II* (Elsevier Science Publishers, Amsterdam, 1991).
- [11] J.R. Gonzalez-Velasco, M.A. Gutierrez-Ortiz et al., *Appl. Catal.* 22 (1999) 167.
- [12] G. Colon, M. Pijolat, F. Valdivieso et al., *J. Chem. Soc., Faraday Trans.* 94 (1998) 3717.
- [13] P.A. Weyrich, H. Trevino, W.F. Holderich and W.M.H. Sachtler, *Appl. Catal.* 163 (1997) 31.
- [14] Z.L. Liu and Y.L. Fu, *Chinese J. Catal.* 22 (2001) 62.
- [15] Z.L. Liu and Y.L. Fu, *J. Mol. Catal. (China)* 15 (2001) 81.
- [16] Y.A. Lokhov and A.A. Davydov, *Kinet. Katal.* 21 (1980) 1093.
- [17] C.M. Grill and R.D. Gonzalez, *J. Phys. Chem.* 84 (1980) 878.
- [18] R. Raval, G. Blyholder, S. Haq et al., *J. Phys. Condens. Matter.* 1 (1989) SB165.
- [19] X. Xu, P. Chen and D.W. Goodman, *J. Phys. Chem.* 98 (1994) 9242.
- [20] T.E. Hoost, K. Otto and K.A. Laframboise, *J. Catal.* 155 (1995) 303.
- [21] K. Almusaiteer and S.S.C. Chuang, *J. Catal.* 180 (1998) 161.
- [22] M. Valden, R.L. Keiski, N. Xiang et al., *J. Catal.* 161 (1996) 614.
- [23] D.W. Goodman, *Chem. Rev.* 95 (1995) 523.
- [24] K. Almusaiteer and S.S.C. Chuang, *J. Catal.* 184 (1999) 189.
- [25] M. Ricken, J. Nölting and I. Riess, *J. Solid State Chem.* 54 (1984) 89.
- [26] R. Korner, M. Ricken, J. Nölting et al., *J. Solid State Chem.* 78 (1989) 136.
- [27] V. Perrichon, A. Laachir, G. Bergeret, et al., *J. Chem. Soc., Faraday Trans.* 90 (1994) 773.
- [28] A. Laachir, V. Perrichon, A. Badri et al., *J. Chem. Soc., Faraday Trans.* 87 (1991) 1601.
- [29] A. Badri, J. Lamotte, J.C. Lavalle et al., *Eur. J. Solid State Inorg. Chem.* 28 (1991) 445.
- [30] A. Badri, C. Binet and J.C. Lavalle, *J. Chem. Soc., Faraday Trans.* 9, 92 (1996) 1603.